Journal of the European Ceramic Society 21 (2001) 785–793

www.elsevier.com/locate/jeurceramsoc

Enhancing the mechanical properties of porcelain stoneware tiles: a microstructural approach

Cristina Leonelli *, Federica Bondioli, Paolo Veronesi, Marcello Romagnoli, Tiziano Manfredini, Gian Carlo Pellacani, Valeria Cannillo

Faculty of Engineering, University of Modena and Reggio Emilia, 41100 Modena, Italy

Received 25 May 2000; received in revised form 30 August 2000; accepted 10 September 2000

Abstract

This paper focuses on the complexities of the microstructure and phase development in porcelain stoneware tiles produced following industrial fast single firing cycles. A microstructural investigation was conducted to determine if the addition of selected low cost minerals would improve mechanical properties. The minerals tested were quartz, mullite and kyanite. Uniaxially pressed samples were submitted to the same industrial firing schedule and tested according to the European tile standards before further microstructural analysis. All the requirements specified in UNI EN normative concerning BIa class tiles were fulfilled; moreover, mullite and kyanite added formulations showed sensible increases in mechanical properties, especially as far as flexural strength and abrasion resistance are concerned. © 2001 Published by Elsevier Science Ltd.

Keywords: Mechanical properties; Microstructure-final; Porcelain; Tiles

1. Introduction

Porcelain stoneware tiles are primarily composed of clay, feldspar and quartz, heat-treated to form a mixture of glass and crystalline phases. Composition variations are negligible and can be presented graphically as a portion of the (Na_2O,K_2O)–Al_2O_3–SiO_2 phase diagram (Fig. 1).[1] Most of the reactions occurring during firing are kinetically governed processes that do not reach thermodynamic equilibrium, since the industrial cycles are as short as 1 h. Hence, it is very common for the finished product to contain crystals of quartz and feldspars that have not been entirely transformed. The plastic clay components, necessary to attain high green densities and advanced densification of the fired product in a single fast firing cycle, disappear completely to give rise to form mullite.[2]

From an economic perspective, porcelain stoneware accounts for 33% of the entire ceramic tiles market world-wide, at sales levels of 119.5 Mm^2 in 1997 and 163.8 Mm^2 in 1998. Moreover, in the last decade the global production, inclusive of porcelain tiles, was oriented mainly towards large formats (less than 25 tiles per m^2), increasing from 42% in 1988 to 82% in 1998.[3] This trend towards producing larger and larger ceramic tiles indicates the need to enhance the mechanical properties of the final product, especially as far as flexural strength is concerned.

Despite the commercial interest in developing porcelain stoneware tiles, very little research has been conducted in the field,[4] leaving significant opportunities for investigation and study, particularly in the two topical areas of phase and microstructure evolution and mechanical performances, which are the main topics of this paper. Within each context, the discussion of porcelain stoneware refers primarily to unglazed tiles and consequently ignores glazing, decorating and polishing issues. The first objective was to follow the phase evolution with temperature in two industrial formulations, which have different mechanical properties. Secondly, the resulting specimens were investigated in order to acquire information linking their microstructural properties and the occurrence of peculiar fracture mechanisms to the development of enhanced mechanical properties. The final portion of the study was aimed at preparing and examining three new compositions, where quartz, mullite and kyanite were added separately to the starting formulations, and the final product experimentally evaluated.

* Corresponding author.
E-mail address: leonelli@mail.unimo.it (C. Leonelli).

0955-2219/01/$ - see front matter © 2001 Published by Elsevier Science Ltd.
PII: S0955-2219(00)00266-1

2. Experimental procedure

Starting formulations were chosen among the numerous varieties in production in the largest Italian ceramic tiles area (Sassuolo, Modena). Two different porcelain stoneware products were selected, the first presenting higher abrasion resistance and being whiter in color, hereafter denoted as SB, and the second higher in modulus of rupture (MOR) value and being brownish in color, denoted as Base. Mineralogical constituents of the two bodies are approximately the same (Table 1) with the exception of zircon, $ZrSiO_4$, which is included in SB.

The grain size distribution of the unfired bodies presents a typical bimodal configuration with the first maximum occurring for clay minerals between 2 and 5 μm and the second maximum at about 10–20 μm for quartz and feldspar. The cumulative curves indicate that 50% of the particles are below 7 μm and that all the particles have diameters below 50 μm.[5]

The unfired mixture of base body composition was then added to 10 wt.% of quartz, mullite and kyanite powders, hereafter indicated as B–Q, B–M, B–K, respectively (Table 2). The mixtures were homogenized in a ball mill with Al_2O_3 milling media for 10 min. Subsequently, the water-based slurry was dried for 12 h and the dried powders were passed through a 125 μm sieve.

All the prepared bodies were formed into tiles by uniaxially pressing the mixture at 33 MPa in a die with a bar shape (110×55 mm). Firing was carried out in a laboratory scale roller gas kiln, with an industrial cycle of total 59 min including cooling, with maximum temperatures of 1160, 1180, 1200 and 1220°C.

The densification behavior was described in terms of water absorption, as required by EN 99, together with linear shrinkage, EN 98. X-ray diffraction, XRD (Philips PW 3710, The Netherlands) spectra of the fired samples were taken at room temperature on the as-obtained surface. The scanning rate was set to 0.02° 2θ per s over a range of 4–60° 2θ, which contained the strongest diffraction-line intensities of clays, quartz, feldspars and mullite. The composition and microstructure of the samples were also based on the result of X-ray fluorescence analyses, as measured by EDS (EDAX CDU LEAP, NY, US), on fired surfaces manually polished through 0.3 μm alumina slurry. Two fundamental measurements of spot and dot mappings were conducted in the polished surfaces analyses, where the accelerating voltage was kept constant at 20 kV. Electrical charging was avoided by gold coating the specimens for scanning electron microscopy, SEM (PSEM XL 40, Philips, The Netherlands). Porosity evaluation on BSE images was performed by using image elaboration software (Image Tool, UTHSCSA, University of Texas, San Antonio, USA). Flexural strength was determined according to EN 100 on 200×100 mm specimens, whilst abrasion resistance was performed using corundum powder abrasive as described in test EN 102. Fracture behavior was investigated in terms of crack pathways as observed by SEM after indentation for 30 s with a static 9.8 N force applied to a Vickers diamond coated indenter held perpendicular to the tile surface (Matzusawza Seiki Co. DMH-2, Tokyo, Japan).

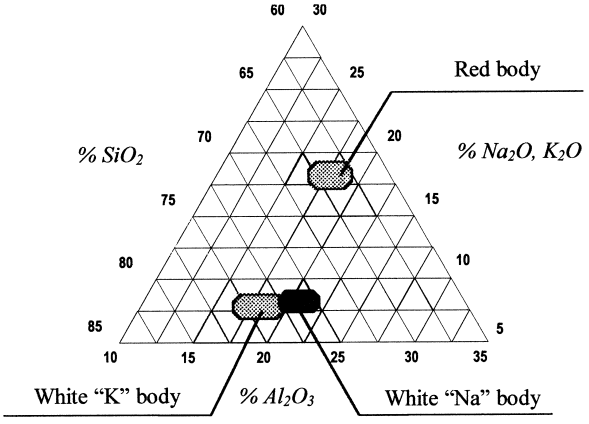

Fig. 1. Visualization of typical porcelain stoneware compositions in the (Na_2O,K_2O)–Al_2O_3–SiO_2 phase diagram.

Table 1
Main mineralogical composition of the two bodies (x indicates relative quantities)

Mineral name	Base	SB
Quartz	xx	xx
Kaolinite	x	xx
Talc	x	x
Illite	xx	x
Potash feldspar	x	x
Sodium feldspar	x	x
Zircon	–	x

3. Results and discussion

3.1. Densification

Densification was monitored by measuring two variables: linear shrinkage and water absorption.

Table 2
Composition and grain size of the added raw materials

	Quartz	Mullite	Kyanite
SiO_2 (wt.%)	99	24.5	38–44
Al_2O_3 (wt.%)	0.5	75	54–60
Fe_2O_3 (wt.%)		0.05	0.4–1.1
Alkaline oxides (wt.%)		0.29	–
Grain size (μm)	20–30	20–30	8–9

The highest shrinkage values were recorded for group SB specimens, presenting the highest kaolinitic clay content with respect to other bodies. Base, mullite and kyanite-added compositions showed lower shrinkage values, and the quartz added one, as expected, resulted the body having the smallest shrinkage (Fig. 2).

The peculiar behavior shown by base body, i.e. an increase in shrinkage from 1200 to 1220°C, indicates overfiring; since this phenomenon is absent in the other compositions, it means that 10 wt.% addition of refractory raw materials, such as the ones used for this study, zircon, quartz, mullite, and kyanite, is sufficient to extend the firing range. At the firing temperature of 1220°C, base, B–Q, B–M, B–K present very similar shrinkage with values approximately 7%, comparable to the industrial range of 5–7.5%.[6]

Water absorption (WA) is the parameter, which according to EN 87, defines the class to which any tile product belongs, so it appears of main importance in the study of densification. As shown in Fig. 3 all the bodies present values well below 0.5% indicating their conformity to EN87 normative class BI (WA < 3%), subclass BIa (WA < 0.3%).

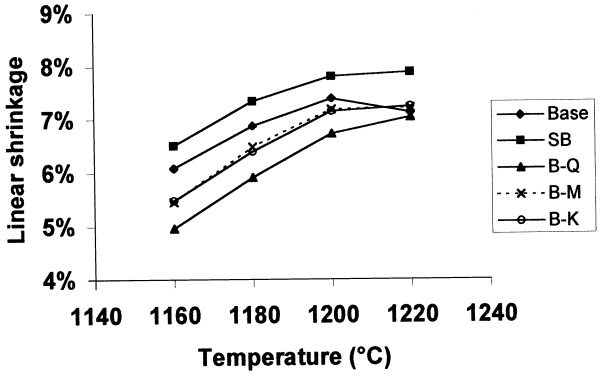

Fig. 2. Linear shrinkage % of the understudied compositions as function of maximum firing temperature (EN 98).

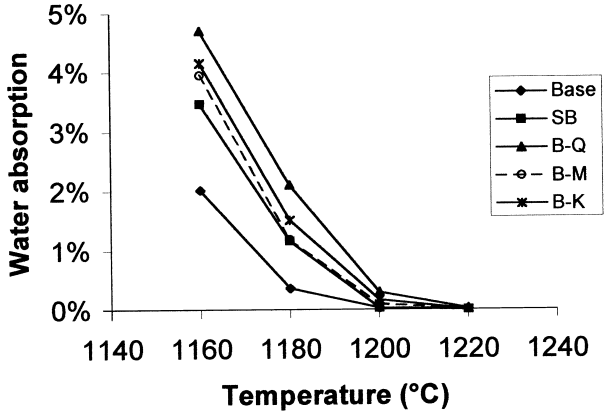

Fig. 3. Water absorption % of the understudied compositions as function of maximum firing temperature (EN 99).

This implies also that the B–Q, B–M, B–K bodies can be classified in the range commercially used for porcelain stoneware as far as water absorption is concerned. As was reported for linear shrinkage, the most refractory body is the quartz-added formulation, followed by those containing kyanite and mullite, and the SB formulation containing zirconia.

3.2. Microstructure

Fig. 4 shows SEM micrographs of a surface polished base specimen.

The micrographs, taken at increasing firing temperatures, show the typical sequence of enhanced densification with increasing temperature, characteristic of all the compositions used in this work. The high porosity is clearly visible at the lowest temperature, and its extent numerically confirmed by image analysis. At higher temperature the pores start to coalesce to form a closed porosity which is reduced in extension from 1200 to 1220°C, with the exception of the base sample. Largest pores have been observed to have a diameter approximately of 15–20 μm. It is the presence of potash feldspar and/or sanidine in the formulations that reduces porosity via viscous-phase sintering and reduces deformation at high temperature, since in the temperature range of 700–1000°C the potassium based glassy phase presents higher viscosity than the sodium-based phase,[7] depending on the sodium: potassium ratio.[8]

The overfiring effect on microstructure was confirmed by SEM observations as reported in Fig. 5, collected at higher magnification than those shown in Fig. 4.

The increase in the number of the smaller pores in proximity of grain boundaries represents evidence of a local increase in structure density, hence possibly recrystallization. Such an effect is not present in the remaining compositions, see for example Fig. 6 where the microstructure of an SB sample is represented.

The BSE image (Fig. 6) demonstrates the presence of white ZrO_2-rich crystals of a size smaller than 2 μm, which were industrially added to the traditional body formulation. Since in the SB body zirconia is present only in the crystalline form of silicate, zircon, it can be deduced that the white dots in Fig. 6 are $ZrSiO_4$ crystals, as confirmed by X-ray diffraction (Fig. 6c). It is interesting to notice that their distribution in the zones among larger crystals make the profile of the latter ones more evident, thus better defining crystals' shapes and distribution. Hence, it is possible to distinguish two different types of large grains (20–30 μm) from their different shade of gray color (Fig. 6b), the darker being identified as mainly composed of Si and O, i. e. quartz, and the brighter one composed of Al, K, Si and O, probably feldspars, since all the clay minerals are characterized by 2–5 μm crystals. It has also been possible to visualize that the pores are mostly

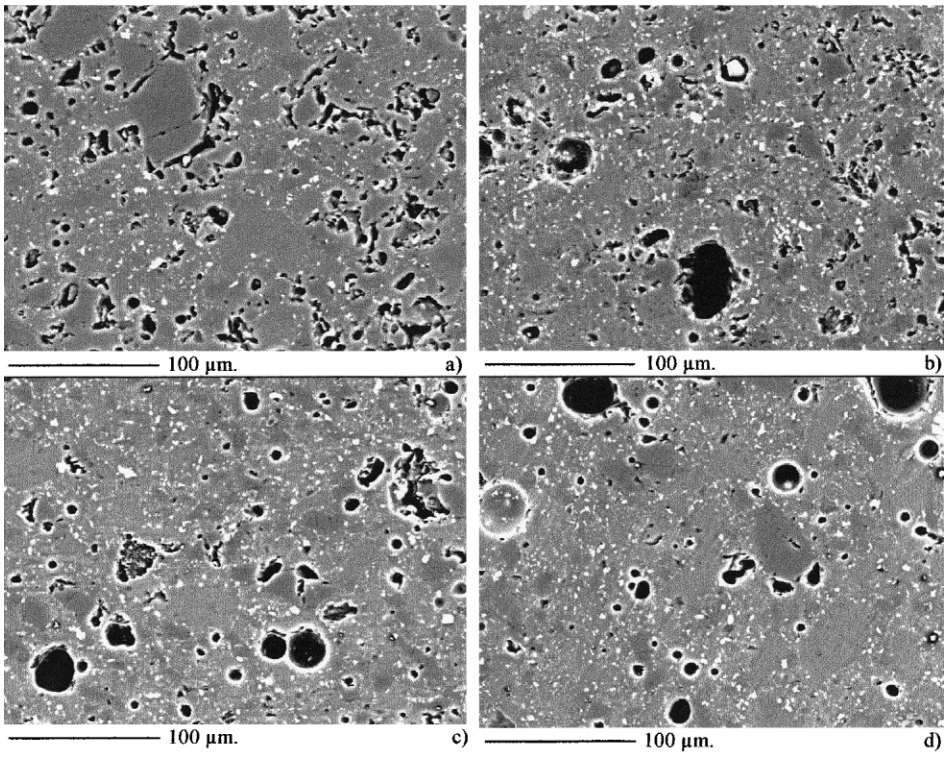

Fig. 4. SEM micrographs of the Base sample fired at (a) 1160°C, (b) 1180°C, (c) 1200°C and (d) 1220°C.

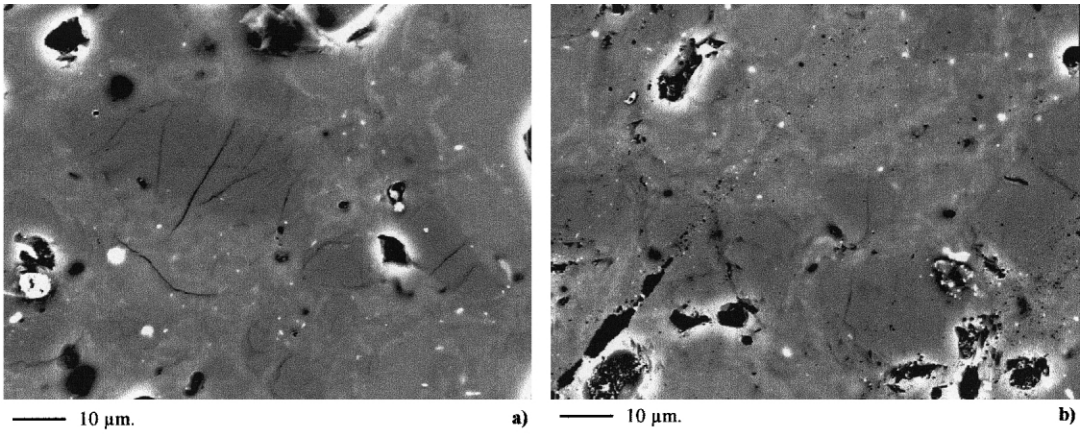

Fig. 5. SEM micrographs of the Base sample fired at (a) 1200°C, (b) 1220°C.

concentrated in the amorphous phase near the grains boundaries.

To better evidence the nature of the different crystalline and amorphous phases the atomic distributions were collected for different elements and presented as distribution maps in Fig. 7. Mg, Ca, Ti, Fe have a homogeneous distribution in all the samples: hence their distribution maps are omitted, whilst K, Na, Al, Si, Zr, are concentrated in different areas indicating different phases. Sodium and potassium are homogeneously dispersed in those areas where silicon presents a minimum concentration, so it can be deduced that they are present in both feldspars and clays, either crystalline or amorphous, while they are completely absent in the quartz crystals. Also aluminum is absent in the areas of highest silicon concentration, again indicating the presence of quartz, but its concentration in the amorphous phase represents a trace of clay reactivity towards the amorphous phase and mullite crystals (see XRD data discussion). Such an amorphous phase is directly formed from the amorphous silica liberated during the metakaolin decomposition which is particularly reactive,[9,10] possibly assisting the eutectic melt at 990°C with potash feldspar[11] and at 1050°C for soda feldspar, according to the K_2O–Al_2O_3–SiO_2 and Na_2O–Al_2O_3–SiO_2 phase diagrams, respectively.[12] Zirconium is concentrated in

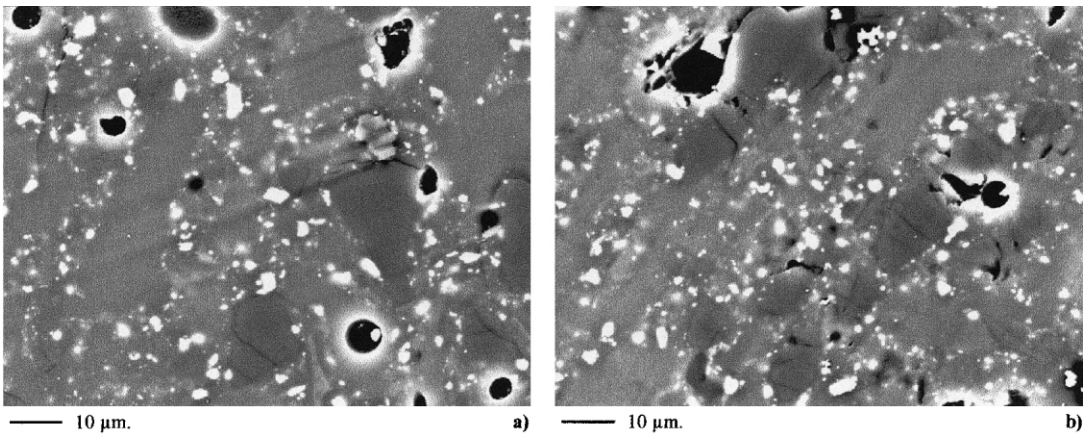

Fig. 6. SEM micrographs of the SB sample fired at (a) 1200°C, (b) 1220°C.

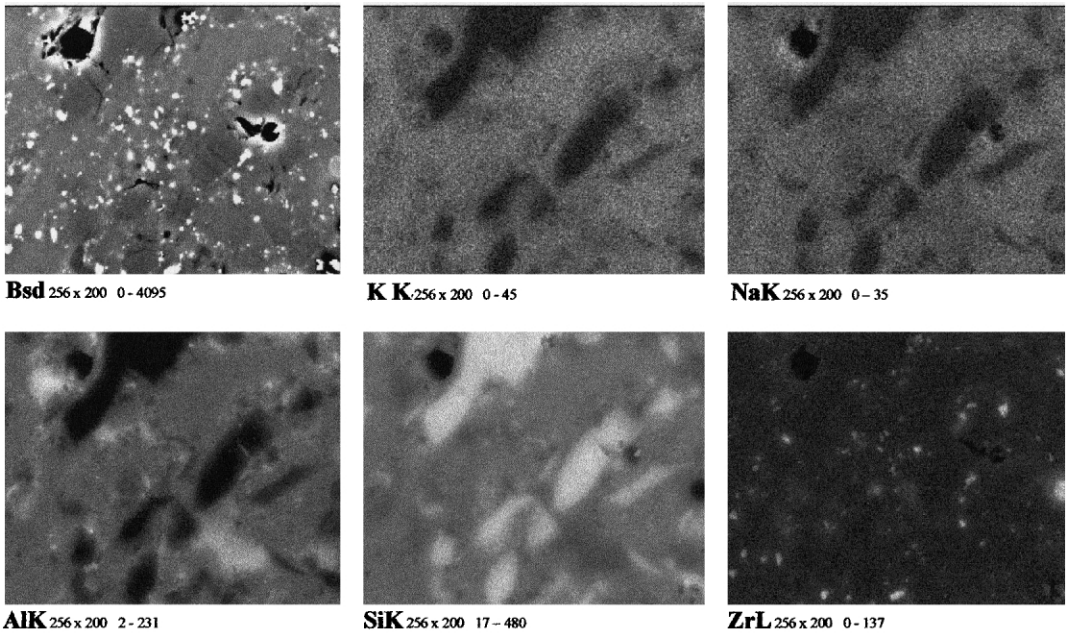

Fig. 7. BSE image (a) and dot maps of the atomic distribution (b) K, (c) Na, (d) Al, (e) Si and (f) Zr of SB sample fired at 1220°C.

the zircon crystals as already described for the BSE image. The distribution map of Al in the overfired Base sample indicates that the amorphous phase is present to a larger extent with respect to the other bodies (Fig. 8). The brighter areas around polygonal shaped grains at two different gray levels indicate that aluminum preferentially migrates in the amorphous phase distributed at grain borders. Morphologies of samples B–Q, B–M, B–K are very similar to those discussed above and are depicted in the BSE images in the following section.

The mullite crystals, approximately 1 μm in size, are present in their characteristic needle-like morphology found in the glassy matrix at a certain distance from quartz, feldspar, mullite and kyanite grains (Fig. 9). This distribution clearly indicates the formation of primary mullite crystals from clay minerals and the contemporary formation of an interfacial glassy layer which is dissolved during etching. An effect similar to that observed by Carty and Senapati[13] for Al_2O_3 grains in porcelain dinnerware exists for $ZrSiO_4$ grains: the oxide favors mullite crystallization on its surface similarly in morphology to alumina in porcelain.

The presence of a sufficiently extended glassy phase capable of wetting all the crystalline phases which remain unchanged during firing allows the comparison between the microstructure of porcelain stoneware and that of porcelain. Hence, the microstructure analyzed in this study can be easily visualized as that of a composite material, where the matrix is represented by the continuous glassy phase and the dispersed particles are identified with crystalline phases, such as quartz, mullite (added or formed during firing), and kyanite.

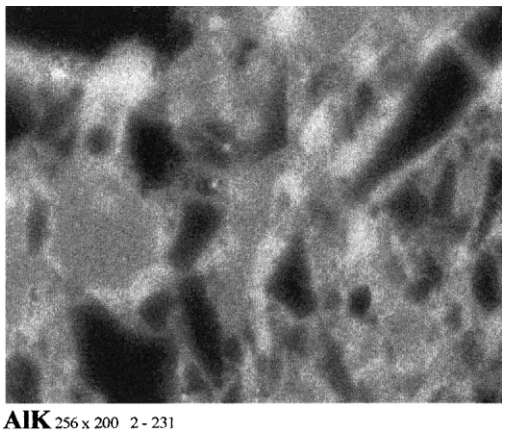

Fig. 8. Dot map of the atomic distribution of Al in the Base sample fired at 1220°C.

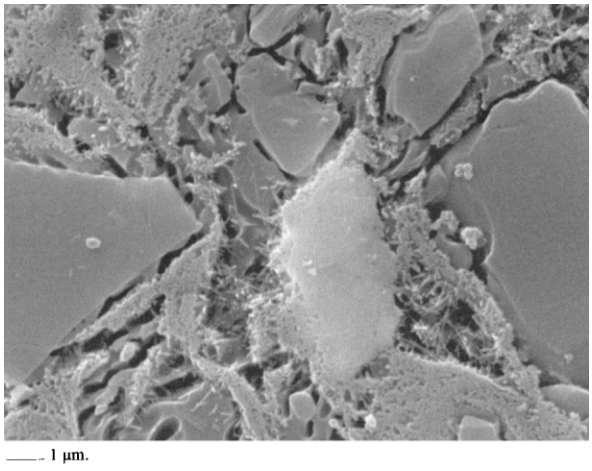

Fig. 9. SEM micrograph after HF etching of SB sample fired at 1220°C.

As far as the identification of the crystalline phases in the fired tiles is concerned, it was observed from XRD patterns that among the starting raw materials in base, SB and B–Q formulations, only quartz remained until the end of the firing cycle, while mullite was the only newly formed crystal.[6] Quartz and mullite were the only two crystalline phases identified also for B–M. For the B–K composition these two main phases were accompanied by kyanite which does not appear to have reacted during the high temperature cycle. Compared with porcelains, porcelain stoneware bodies generally contain a single mullite, $3Al_2O_3.2SiO_2$, evolution pathway: the dehydroxylated kaolin, metakaolin, transforms into a nonequilibrium unstable spinel type structure, which converts to mullite above 1075°C.[13]

3.3. Mechanical properties and fracture analysis

Flexural strength of the fired tiles was examined in terms of modulus of rupture (MOR) as a function of maximum firing temperature (Fig. 10). The mechanical

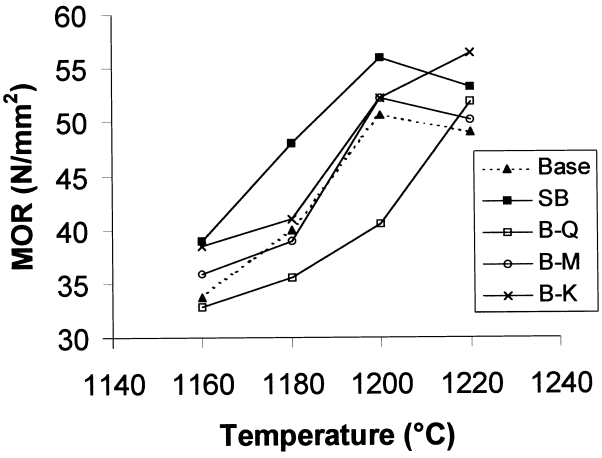

Fig. 10. Modulus of rupture of the understudied composition as a function of maximum firing temperature.

behavior is quite similar for all the compositions, i.e. MOR values increase with densification, with the base body having the lowest MOR values and the B–K the sample groups having the highest values. At the maximum firing temperature the average MOR values are between 30 and 50 N/mm^2, being acceptable according to EN 100 that requires values higher than 27 N/mm^2.

The strength of porcelain has been explained by developing three major theories[13] that can be summarized in the mullite hypothesis[14] (the feltlike interlocking of fine mullite needles are responsible for the porcelain strength), the matrix reinforcement (induced "thermal" compressive stresses due to thermal expansion mismatch lead to strength improvement) and the dispersion-strengthening hypothesis (the dispersed particles limit the size of Griffith flaws, leading to increased strength). In order to determine which of these hypothesis can be applied to the case of porcelain stoneware, further observations were performed to evaluate some micromechanics phenomena during crack propagation after indentation at 9.8 N static load on the polished surface of the 1220°C treated samples. Micrographs of cracks developed in the base and SB samples are shown in Fig. 11. In all the images the stressed and cracked quartz grain are clearly visible, as indicated by the arrows, at the magnification used for these observations.

The average quartz grain size being between the limit described by Warshaw and Seider[15] of 25 to 50 μm for little peripheral fracture and rare matrix fractures, the quartz crystals react to crack propagation with a microcracking toughening mechanism.[16] Typically this mechanism is visible in the studied samples as crack branching (Fig. 11a) at the impact of the crack with a quartz grain. Such artifacts, induced by specimen preparation, were well explained for porcelain bodies by Carty and Senapati.[13] Also crack deflection is observed as a crack propagation mechanism in the proximity of

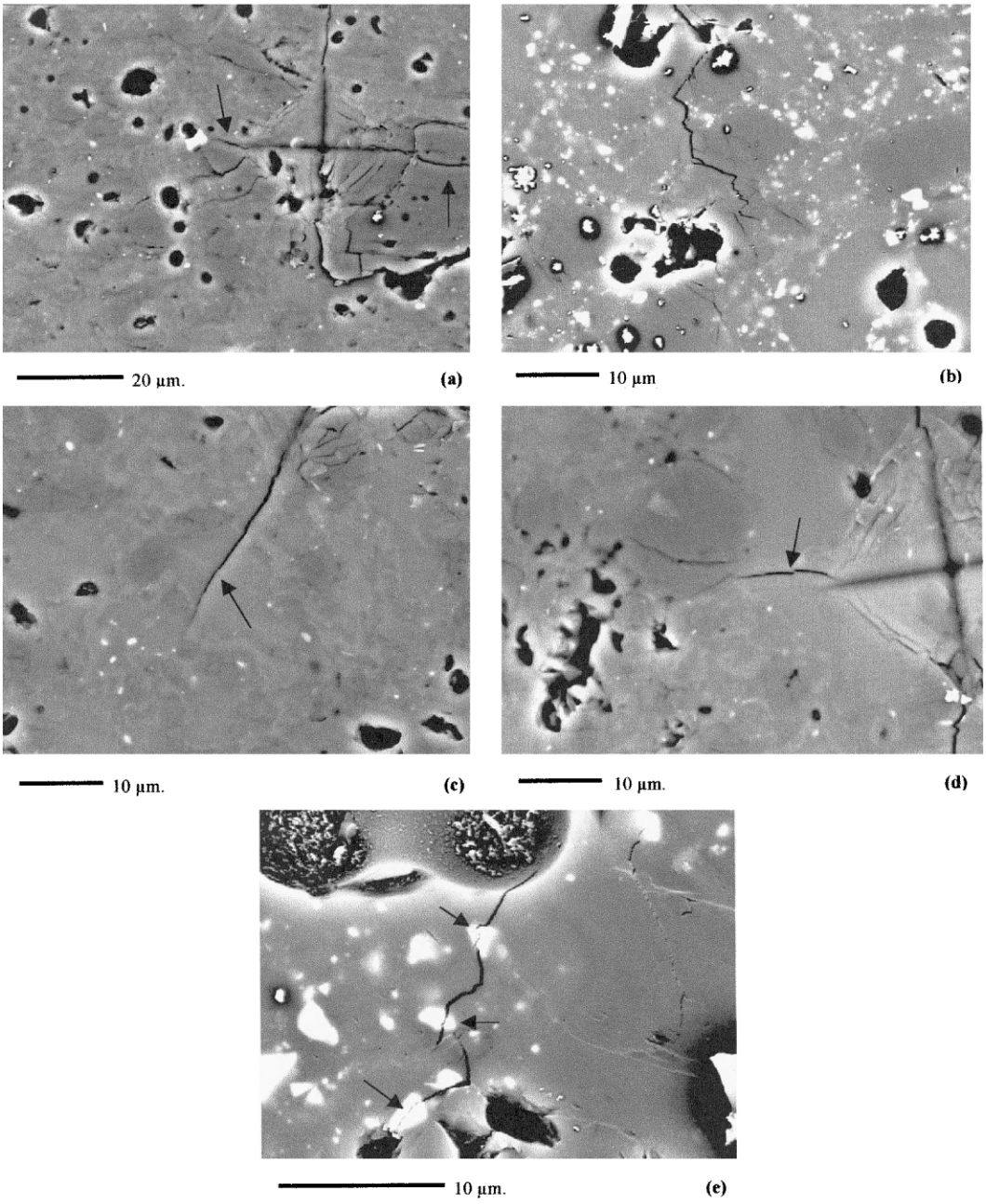

Fig. 11. SEM micrographs of cracks in Base and SB samples after indentation.

the quartz crystals (Fig. 11b). When the crack propagates through a feldspar grain (Fig. 11c and d), it does not deviate from its path until when it meets a stressed quartz grain; energy is dissipated and propagation stopped. In the SB samples the crack deflection by zirconia grains is not efficient in stopping the crack, which propagates through three grains (Fig. 11e), demonstrating the effect of the lower flexural strength of the composition, as reported in Fig. 10. Also B–M and B–K samples present only a crack deflection mechanism via mullite and kyanite crystals (Fig. 12).

The dispersion-strengthening hypothesis[17–21] may be confirmed here since strength increase is correlated to mullite and kyanite particles, that are stronger than prestressed quartz. Abrasion resistance tests were performed in order to show any enhancement in such a mechanical property due to the presence of hard particles bonded to the matrix by a good interface. Such bonding was identified as the glassy phase shown in the SEM micrographs.

The abrasion resistance of the as-fired tiles was checked according to EN 102 and measured in terms of removed sample volume (Fig. 13). The values are all similar and located in the range 75–90 mm^3 for the samples fired at higher temperature, according to the maximum densification reached. B–K and B–M samples

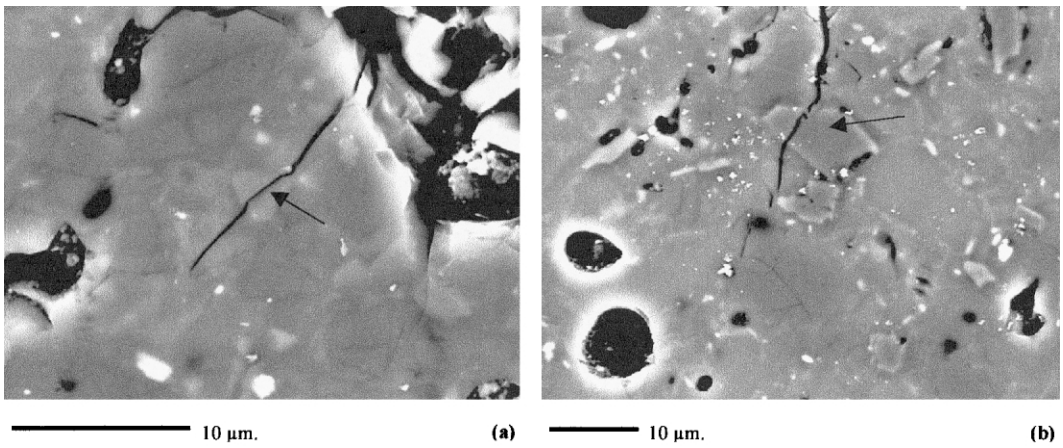

Fig. 12. SEM micrographs of crack deflection in (a) B–M and (b) B–K samples after indentation.

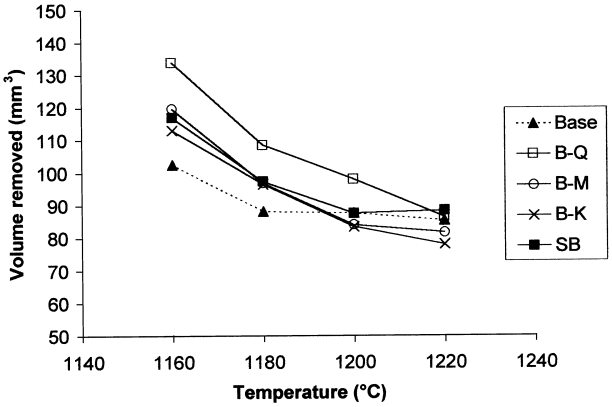

Fig. 13. Volume removed during abrasion test as function of maximum firing temperature (EN 102).

present the lowest values of abraded volume, thus confirming the presence of a good interface produced with the glassy phase.

4. Conclusions

The addition of raw materials to a base formulation of industrial porcelain stoneware lead to ceramic tiles which possess all the requirements specified in UNI EN normative.

The mechanism of crack propagation suggests several possible toughening processes which are common for porcelain bodies as well.

The increase in flexural strength for the mullite and kyanite containing formulations seems due to the presence of a more reactive interface which is evident in the micrographs as an amorphous layer surrounding the polygonal shapes typical of such unreacted crystals.

This study suggests the possibility of designing compositional variation to enhance and control mechanical properties of porcelain stoneware on the basis of the experimental results obtained by applying methodologies used for traditional ceramics and composite materials.

Acknowledgements

We would like to thank Prof. Licio Pennisi for many stimulating discussions and Paolo Gafforio for experimental assistance.

References

1. Ravagli, M. and Fiori, C., The use of microgranites in the porcelain stoneware tile production. *Ceramica Informazione*, 1993, **330**, 538–546.
2. Schüller, K. H. *Process Mineralogy of Ceramic Materials; Chapter. 1*. W. Baumgart. Ferdinand Enke, Stuttgart, Germany, 1984.
3. Biffi, G., Workshop on porcelain stoneware tile, Modena 10th June 1999. *Ceramica Informazione*, 1999, **391**, 659–668.
4. Descamps, P., Tirlocq, J., Deletter, M. and Cambier, F. The composite approach for the reinforcement of ceramic floor tiles.

In: *Procedings of Qualicer 2000*, p. P.GI 379-394, Castellon, Spain, 2000.
5. Gafforio, P., Correlation between microstructure and mechanical properties of porcelain stoneware. Bachelor thesis, University of Modena, 1997.
6. Manfredini, T., Pellacani, G. C. and Romagnoli, M., Porcelainized stoneware tile. *Am. Ceram. Soc. Bull.*, 1995, **74**, 77–79.
7. Varshneya, A. K., *Fundamentals of Inorganic Glasses*. Academic Press, San Diego, 1994 p. 197.
8. Lundin, S. T., Microstucture of porcelain. In: M*icrostructure of Ceramic Materials*, Vol. 257, NBS Misc. Publications, 1964, pp. 93–106.
9. Okada, K., Otsuka, N. and Ossaka, J., Characterisation of spinel phase formed in the kaolin-mullite thermal sequence. *J. Am. Ceram. Soc.*, 1986, **69**(10), C-251–C-253.
10. Sonuparlak, B., Sarikaya, M. and Aksay, I. A., Spinel phase formation during 980°C exothermic reaction in the kaolinite-to-mullite reaction series. *J. Am. Ceram. Soc.*, 1987, **70**(11), 837–842.
11. Kingery, W. D., *Introduction to Ceramics*. Wiley, NY, 1976.
12. Levin, E. M., Robbins, C. R. and McMurdie, H. F., Figs. 407 and 501. In *Phase Diagram for Ceramist* ed. M. K. Reser. American Ceramic Society, Columbus, Ohio, 1964.
13. Carty, W. M. and Senapati, U., Porcelain-raw materials, processing, phase evolution, and mechanical behavior. *J. Am. Ceram. Soc.*, 1998, **81**(1), 3–20.
14. Mattyasovszky-Zsolnay, L., Mechanical strength of porcelain. *J. Am. Ceram. Soc.*, 1957, **40**, 299–306.
15. Warshaw, S. I. and Seider, R., Comparison of strength of triaxial porcelains containing alumina and silica. *J. Am. Ceram. Soc.*, 1967, **50**, 337–343.
16. Rice, R., Processing of ceramic composites. In Advanced Ceramic Processing and Technology, Vol. 1, ed. J. G. P. Binner. Noyes Publications, Park Ridge, NY, US, 1990.
17. Maity, S. and Sarkar, B. K., Development of high-strength whiteware bodies. *J. Eur. Ceram. Soc.*, 1996, **16**, 1083–1088.
18. Maity, S., Mukhopadhyay, T. K. and Sarkar, B. K., Sillimanite sand-feldspar porcelains: I. Vitrification behavior and mechanical properties. *Interceram*, 1996, **45**, 305–312.
19. Blodgett, W. E., High strength alumina porcelains. *Am. Ceram. Soc. Bull.*, 1961, **40**, 74–77.
20. Harada, R., Sugiyama, N. and Ishida, H., Al_2O_3-strengthened feldspathic porcelain bodies: effects of the amount and particle size of alumina. *Ceram. Eng. Sci. Proc.*, 1996, **17**, 88–98.
21. Davidge, R. W., Mechanical behavior of ceramics. Cambridge Solid State Series, Cambridge University Press, pp. 87–88.